Journal of Physics: Conference Series **2374** (2022) 012107 doi:10.1088/1742-6596/2374/1/012107

Charged particle identification performance of the TOP counters in Belle II

S. Sandilya [†1], A. Schwartz [2], and U. Tamponi [3]
(On behalf of the TOP group in the Belle II collaboration)

[1] Indian Institute of Technology Hyderabad, Telangana 502285, India
[2] University of Cincinnati, Cincinnati, Ohio 45221, USA
[3] INFN - Sezione di Torino, I-10125 Torino, Italy

E-mail: [†]saurabh@phy.iith.ac.in

Abstract. The Time-Of-Propagation (TOP) counter is a novel ring-imaging Cherenkov detector that primarily consists of a quartz bar radiator, micro-channel plate photomultipliers and front-end readout electronics. These TOP counters are installed in the central region of the Belle II detector to provide the crucial information on the charged particle identification (PID). Here, we present an overview of PID studies in Belle II, with a focus on the performance of the TOP detector. The results presented are from the recently recorded data which show reasonable agreement with the expectations from the simulation studies.

1. Introduction

An efficient PID is desired in almost all the particle physics experiments for identifying the final state particles from a decay of interest [1]. Particularly, for a B-factory experiment such as Belle II, the PID information is essential for determining the flavor of the B mesons [2].

The Belle II detector [3] is located around the interaction region (IR) of SuperKEKB [4] asymmetric-energy e^+e^- collider in KEK, Tsukuba, Japan. Belle II is composed of several sub-detectors arranged in cylindrical geometry around the IR. The sub-detectors installed specifically to obtain PID information are : the TOP counters in the central region and Aerogel Ring Imaging Cherenkov (ARICH) counters [5] in the forward region (in the direction of the incoming e^- beam). The central drift chamber (CDC) is the tracking device of Belle II, which also contributes to the PID by providing the measurement of the specific ionization loss by the traversing charged particle. The acceptance regions of CDC, TOP and ARICH in polar angle ($\cos\theta$) are $[-0.87, 0.96]$, $[-0.48, 0.82]$, and $[0.83, 0.97]$, respectively.

We report the overall PID performance of Belle II with focus on the TOP detector. The PID performance assessment is based on 71.2 fb^{-1} data recorded at and near (below 60 MeV) the $\Upsilon(4S)$ resonance peak. (Inclusion of charge-conjugate processes is implied throughout this article.)

2. The TOP Detector

The TOP detector consists of 16 modules arranged in a barrel shape array with an inner radius of about 1.2 m. Each of the TOP module primarily consist of a quartz radiator bar, micro-channel plate photomultipliers (MCPPMTs) and a front-end readout. The schematic of

a TOP module is depicted in figure 1. The quartz radiator in TOP is formed by epoxying two quartz bars each with dimension: $(1250 \times 450 \times 20)$ mm^3, an expansion volume with dimension: $(100 \times 456 \times 20 - 51)$ mm^3, and a mirror with dimension: $(100 \times 450 \times 20)$ mm^3.

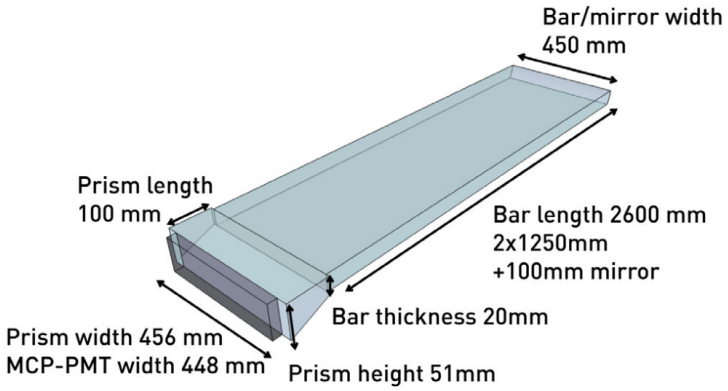

Figure 1. Schematic of a TOP module.

When a relativistic charged track passes through the quartz radiator bar (which acts as a dielectric medium) exceeding the speed of light in the radiator, Cherenkov photons are emitted at a characteristic angle which depends on the velocity of the traversing charged particle. These Cherenkov photons propagate in the quartz radiator bar through total internal reflections preserving the emission angle. The mirror at the rear end has a radius of curvature of about 6500 mm, which is mounted to reduce the effect of bar thickness and correct for the chromatic dispersion [7]. The refractive index of the radiator is about 1.44 with high bulk transmittance and internal reflectance to minimize the loss of number of photons during propagation or reflections [6]. The expansion volume end of the quartz radiator bar is coupled with an array of two rows of 16 MCPPMTs (32 MCPPMTs per module) forming a photo-detection plane, where the Cherenkov photon get registered. Each MCPPMT is square-shaped, and have an effective area of (23×23) mm^2, which is segmented into 16 channels [8][9]. Charged particle of different masses (for example K's and π's) but with same momenta (determined from CDC) will have different velocity and hence different time-of-flight and characterstic angle of Cherenkov photon [10][11]. The arrival time of photon includes both information: the propagation time of the photon in the quartz bar and the time-of-flight of the charged track from the collision interaction point to the TOP. Ultimately, the photon hit position in the detection plane is combined with the time of arrival to obtain a likelihood for a given particle mass hypothesis [10][11]. The front-end electronics to read out the signals from MCPPMTs is described in the reference [12]. And, lastly each TOP modules are placed in an individual enclosure made of aluminum honeycomb panels, mainly for the structural support.

3. PID performance

We report the PID performance of the charged kaon and pion separation using $D^{*+} \to D^0[K^-\pi^+]\pi^+$ decays. Slow pions, (directly produced from theD^{*+} decays) can be used to tag the flavor of D^0. The kinematically tagged D^0 is ultimately used to identify the kaons and pions by their charge in data.

The decay $D^{*+} \to D^0[K^-\pi^+]\pi^+$ is reconstructed from the charged particles originating from a region near the e^+e^- interaction point. This region is defined using impact parameters: we require $dr < 2$ cm in the x-y plane (transverse to the positron beam), and $|dz| < 4$ cm along the z axis (anti-parallel to the positron beam). Two opposite signed tracks with kaon and pion mass hypothesis are combined to reconstruct a D^0 meson candidate. Another charged track with

pion mass hypothesis (slow pion candidate) is added to reconstruct D^{*+} meson candidate. The momentum of the D^{*+} candidate in the e^+e^- CM frame ($P^*_{D^{*+}}$) is required to be > 2.5 GeV/c, which is useful in selecting the D^{*+} candidates originating from the $e^+e^- \to c\bar{c}$ continuum process. A criterion $|\Delta M - 0.14543| < 1.5\,\mathrm{MeV/c^2}$ is applied to suppress the remaining background events, where ΔM is the difference between reconstructed invariant masses of D^{*+} and D^0 candidates. Lastly, the signal yield is extracted by performing an unbinned maximum likelihood fit to reconstructed invariant mass distribution of D^0 candidates.

The kaon identification efficiency is defined as:

$$\frac{\text{number of kaon tracks identified as kaon}}{\text{number of kaon tracks}};$$

while the pion mis-identification rate is defined as:

$$\frac{\text{number of pion tracks identified as kaon}}{\text{number of pion tracks}}.$$

Information from each PID system is analyzed independently to determine likelihoods $\mathcal{L}_K$ and $\mathcal{L}_\pi$ for K and π hypotheses, respectively. These likelihoods may then be used to construct a combined likelihood ratio $\mathcal{R}_{K/\pi} = \mathcal{L}_K/\mathcal{L}_K + \mathcal{L}_\pi$. The distribution for binary PID likelihood ratio ($\mathcal{R}_{K/\pi}$), can be obtained for signal kaons and pions using ${}_s\mathcal{P}lot$ technique [13] in data. For kaon-like tracks the $\mathcal{R}_{K/\pi}$ value should be towards one, whereas for the pion-like tracks, should be towards zero. For kaon and pion signal tracks, the $\mathcal{R}_{K/\pi}$ distribution in data is shown in figure 2 from all sub-detectors (left) and TOP (right) only information. The $\mathcal{R}_{K/\pi}$ distribution shows clear separation between the kaon and pion tracks.

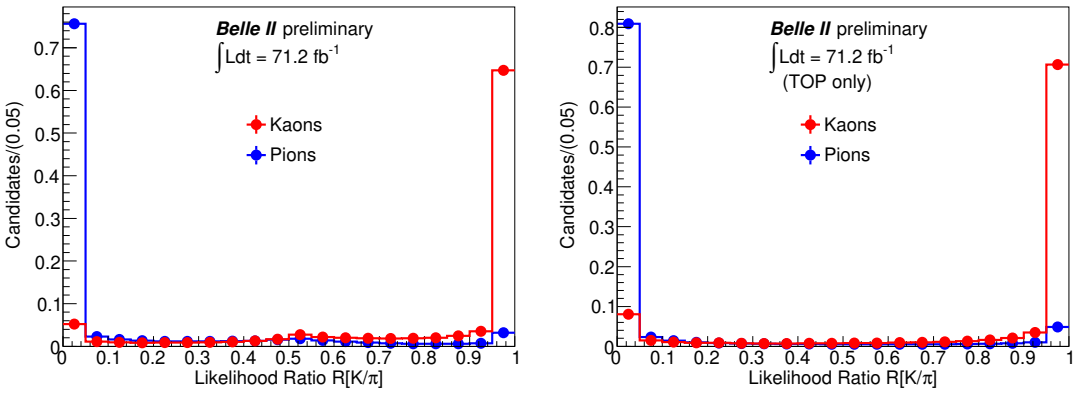

Figure 2. $\mathcal{R}_{K/\pi}$ distributions, for all sub-detectors (left) and TOP only (right), obtained using ${}_s\mathcal{P}lot$ technique for kaon (red) and pion (blue) signal tracks in the data sample.

The K and π from D^0 have a broad momentum distribution around 1-2 GeV/c and then slowly decline towards 5 GeV/c. And, The polar angle distribution of both K and π are populated towards the forward region or $cos\theta \sim 1$. K efficiency and π mis-identification rate for a specific PID criterion $\mathcal{R}_{K/\pi} > 0.5$ in bins of momentum are shown in figure 3 from all sub-detectors (left) and TOP (right) only information. For momenta up to 2 GeV/c the PID K-efficiency about 90% and π mis-identification rate about 5% from TOP only and then the PID performance degrades towards the higher momentum region. However, a good $K-\pi$ separation is maintained at higher momentum region by including information from CDC and ARICH information.

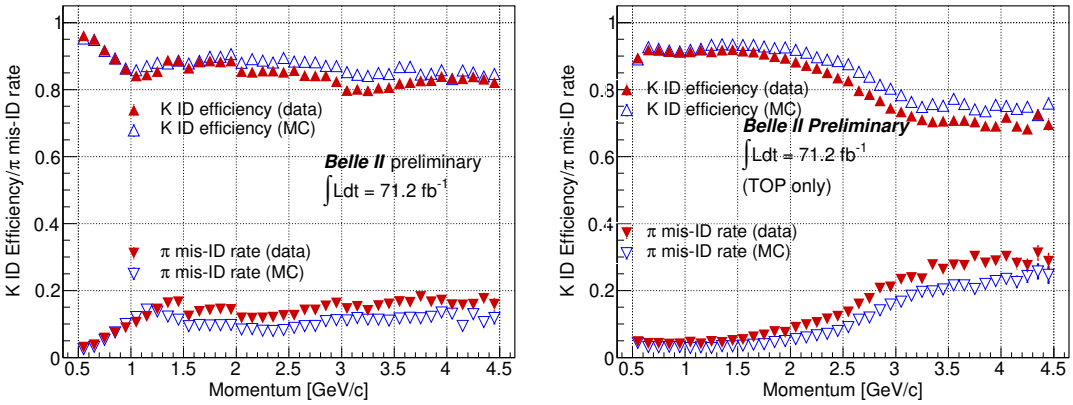

Figure 3. Kaon efficiency and pion mis-ID rate for the PID criterion $\mathcal{R}_{K/\pi} > 0.5$ using the decay $D^{*+} \to D^0[K^-\pi^+]\pi^+$ in the bins of laboratory frame momentum of the tracks from all sub-detectors (left) and TOP only (right).

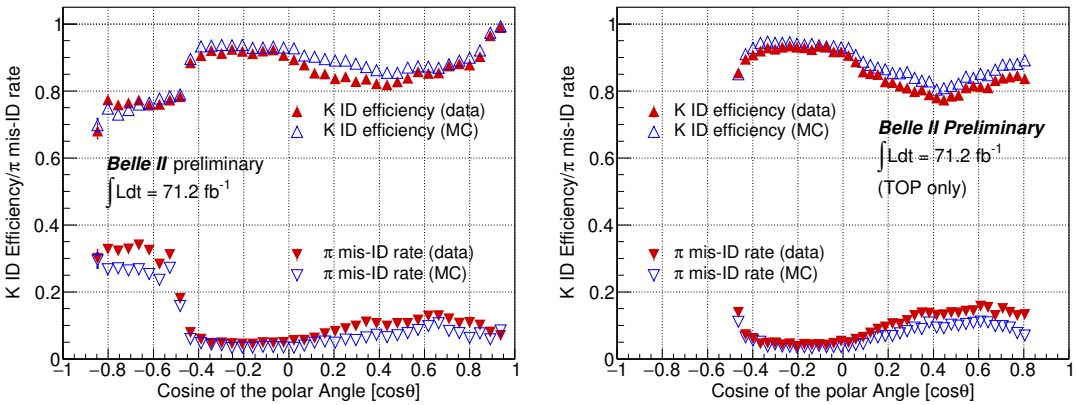

Figure 4. Kaon efficiency and pion mis-ID rate for the PID criterion $\mathcal{R}_{K/\pi} > 0.5$ using the decay $D^{*+} \to D^0[K^-\pi^+]\pi^+$ in the bins of polar angle from all sub-detectors (left) and TOP only (right).

The K efficiency and π mis-identification rates for $\mathcal{R}_{K/\pi} > 0.5$ in polar angle ($\cos\theta$) bins are shown in figure 4 from all sub-detectors (left) and TOP (right) only information.

K identification efficiency and π mis-identification rate from TOP only information for the criterion $\mathcal{R}_{K/\pi} > 0.5$ is calculated in the bins of azimuthal angle, each bin representing a TOP slot, is shown in figure 5. The K efficiency distribution is almost uniform in all the TOP slots around 85%. The TOP modules installed with the conventional MCPPMTs $\phi \in (-2.75, 0)$ have slightly larger π mis-identification rate of about 12% compared to 9.5% in other modules with the lifetime extended MCPPMTs.

4. Summary

An effective and efficient PID for the charged particles up to momenta 4 GeV/c is vital to the physics goals of the Belle II experiment. TOP Detector provides the PID information to the tracks in central and forward region of the Belle II detector. Belle II is recording the e^+e^- collision data smoothly even amid CoViD-19 pandemic. The PID performance of TOP is evaluated with the early recorded data sample. A K identification efficiency of about 85%

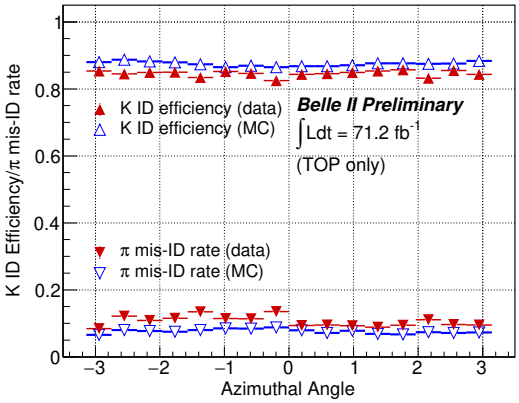

Figure 5. $\mathcal{R}_{K/\pi}$ distributions, for all sub-detectors (left) and TOP only (right), obtained using ${}_s\mathcal{P}lot$ technique for kaon (red) and pion (blue) signal tracks in the data sample.

ia achieved from TOP only information with kinematically tagged D^0 decays with a nominal π mis-identification rate of about 9.5%. There are minor disagreement with simulations (about 3%). The present PID performance of TOP (and Belle II) is expected to improve further in near future as several studies are in progress in this direction.

References

[1] E. Kou et al. (Belle II Collaboration), *Prog. Theor. Exp. Phys.*, Vol. 2019 Issue 12, 123C01 (2019).
[2] F. Abudinen, C. Kiesling, and T. Kuhr, BELLE2-PTHESIS-2018-003 (2018).
[3] T. Abe (Belle II Collaboration), arXiv:1011.0352, Tech. Rep. (2010).
[4] K. Akai et al. (SuperKEKB Collider), *Nucl. Instrum. Methods Phys. Res., Sect.* A **907** 188–199 (2018).
[5] M. Yonenaga et al. *Prog of Theor and Exper Physics*, Vol. 2020, Issue 9, 093H01 (2020).
[6] B. Wang *Nucl. Instrum. Methods Phys. Res., Sect.* A **766** 204–207 (2014).
[7] K. Inami, *Nucl. Instrum. Methods Phys. Res., Sect.* A **595** 96–99 (2008).
[8] M. Akatsu et al. *Nucl. Instrum. Methods Phys. Res., Sect.* A **528** 763–775 (2004).
[9] K. Matsuoka *Nucl. Instrum. Methods Phys. Res., Sect.* A **732** 357–360 (2013).
[10] B. Ratcliff, and J. Vavra, *Nucl. Instrum. Methods Phys. Res., Sect.* A **970** 163442 (2020).
[11] M. Starič, *Nucl. Instrum. Methods Phys. Res., Sect.* A **639** 252–255 (2011).
[12] D. Kotchetkov et al. *Nucl. Instrum. Methods Phys. Res., Sect.* A **941** 162342 (2019).
[13] M. Pivk, and F. R. Le Diberder, *Nucl. Instrum. Methods Phys. Res., Sect.* A **555** 356–369 (2005).